RSC Advances

PAPER

View Article Online
View Journal | View Issue

Cite this: *RSC Adv.*, 2020, **10**, 30825

A deep-red fluorescent molecular rotor based on donor-two-acceptor modular system for imaging mitochondrial viscosity†

Xiaoxi Yin,‡[ab] Yiping Cai,‡[ab] Songtao Cai,[ab] Xiaojie Jiao,[ab] Chang Liu,[ab] Song He*[ab] and Xianshun Zeng *[ab]

Received 4th June 2020
Accepted 28th July 2020

DOI: 10.1039/d0ra04935b

rsc.li/rsc-advances

A new donor-two-acceptor modular fluorescence rotor **DpCy7** involving a phenolate donor unit and two benzothiazolium acceptor moieties was designed and synthesized. The **DpCy7** underwent an internal charge transfer to form a Cy7-like longer conjugated system fluorochrome at a physiological pH. The probe exhibited a strong turn-on (8.5-fold) deep-red emission with a larger Stokes shift in glycerol aqueous solutions with restriction of rotation. Both the fluorescence intensity and fluorescence lifetime displayed the linear relationship of viscosity changes in the logarithmic plots. Furthermore, the HeLa cell imaging experiments of **DpCy7** indicated that the rotor could be used to monitor the mitochondrial viscosity in living cells. This new type of deep-red fluorescence rotor provides a potential platform for determining viscosity at subcellular levels.

Introduction

Fluorescence molecular dyes have emerged as indispensable carriers for imaging techniques for labelling and detecting the biomolecular behavior in chemical reactions or biological processes.[1] Relying on the fluorescence changes of dyes, the specific analytes or the microenvironment parameters are determined by use of fluorescence imaging microscopy with high sensitivity, high spatial-resolution and vivid visibility at the organism and cell levels.[2] Such fluorescence dyes are required to have high quantum yields of fluorescence, long emission wavelengths, large Stokes shifts, and good physiological and photo stability.[3] Furthermore, in order to design fluorescence dyes for *in vivo* imaging, there is a demand for developing deep-red/near-infrared (NIR) fluorescence dyes due to the fact that deep-red/NIR photons can penetrate deeply into tissue with less damage to biological samples and tissue autofluorescence can be significantly lower in the deep-red/NIR emission range.[4]

To date, much effort has been made to synthesize various deep-red/NIR fluorescence dyes. The deep-red/NIR molecular frameworks, commonly based on coumarin,[5] borondipyrromethane[6] (BODIPY), xanthene[7] or cyanines,[8] have been modified as suitable agents for biomedical imaging. Among them, polymethine cyanines are one of most widely used deep-red/NIR platforms with perfect photophysical properties and outstanding biocompatibility.[9] The polymethine carbocyanine dyes typically have a donor–acceptor π electron system (D–π–A) between two nitrogen atoms.[10] Recently, a novel class of turn-on NIR cyanine-like probes based on a donor-two-acceptor (D2A) π electron system was established by incorporating an aromatic ring into the *meso*-position of the polymethine line.[11] These D2A modular fluorescence probes with large Stokes shifts have the advantage of allowing functionalization to mask their fluorescence and release the active dye through the intramolecular charge transfer (ICT) mechanism after the removal of the masker by an analyte.[11a] Hence, this is useful for the development of the D2A cyanine-like modular probes as attractive deep-red/NIR fluorescence probes for biological microenvironment imaging.

Viscosity in the mitochondria is one of the most important factors of the intracellular microenvironment.[12] The abnormal changes of viscosity in mitochondria can influence the substance exchange and diffusion in the cytoplasm, such as transportation of nutrients and metabolic wastes, which subsequently lead to many serious diseases, *e.g.*, Alzheimer's disease, hyperlipidemia, cerebral infarction, and heart disease.[13] Thus, an effective method for the measurement microviscosity is necessary. A series of deep-red/NIR fluorescence molecular rotors were designed to map the viscosity of intracellular locations. Among them, *meso*-substituted symmetrical cyanine dyes,[9a,14] especially pentamethine cyanines (Cy5) and heptamethine cyanines (Cy7), are frequently chosen as deep-red/NIR fluorescence probes for tracking mitochondrial

[a]*Tianjin Key Laboratory for Photoelectric Materials and Devices, Tianjin University of Technology, Tianjin 300384, China. E-mail: hesong@tjut.edu.cn; xshzeng@tjut.edu.cn; Tel: +86-22-6021-6748*

[b]*Key Laboratory of Display Materials and Photoelectric Devices, Ministry of Education, School of Materials Science & Engineering, Tianjin University of Technology, Tianjin 300384, China*

† Electronic supplementary information (ESI) available. See DOI: 10.1039/d0ra04935b

‡ These authors contributed equally to this work.

viscosity due to not only their cationic nature but also because of their larger π-conjugated system.[15] Such molecular rotors typically have freely rotated C–C single bonds connecting the cation dye region and the long conjugated polymethine line. In non-viscous environments, the faster rotation of these C–C single bonds relaxes, and the excited energy results in obvious quenching of fluorescence, whereas in a viscous medium, the rotation is gradually inhibited, thereby increasing the fluorescence intensity. Even though most fluorescence turn-on rotors have been applied to monitor intracellular viscosity, there is still a demand for more sensitive, more versatile fluorescent molecule rotors. As mentioned previously, the D2A cyanine-like probes are logical candidate probes. They could exhibit similar optical behavior to classical cyanine dyes upon removal of a specific mask moiety by an analyte. However, as far as is known, few D2A type fluorescence dyes have been reported as molecular rotors with a sensitive response to the viscosity change of mitochondria.

In this work, a novel deep-red fluorescence molecular rotor **DpCy7** was prepared by condensation of 2,4-diphenoldialdehyde **1** with two equivalents of benzothiazolium iodide molecules (Scheme 1). The **DpCy7** rotor involved a D2A module composed of a diphenol moiety as a latent electron donor and two benzothiazolium groups as electron acceptors. Under physiological conditions, the masked **DpCy7** was activated by deprotonation of one phenol (Scheme 2). The newly formed Cy7-like rotor was sensitive to viscosity and showed a desirable turn-on deep-red fluorescence (8.5-fold) because of the restriction of rotation. Furthermore, the **DpCy7** probe was mitochondria-targetable and was used to study the fluctuations of mitochondrial viscosity in cells stimulated by monensin or nystatin.

Results and discussion

Synthesis of the protonated DpCy7

In order to improve the cell-membrane permeability and enhance the rotary efficiency of the dye, a diphenol moiety was chosen as an efficient electron donor and the *N*-ethylbenzothiazole unit as the electron-withdrawing group. As shown in Scheme 1, isophthalaldehyde **1** was prepared by formylation of 2-methylresorcinol using formamidine acetate and acetic anhydride (Ac_2O) according to a previously reported procedure.[16] Then the molecular rotor **DpCy7** was obtained using a condensation reaction between isophthalaldehyde **1** and benzothiazolium iodide **2**. The anion exchange was achieved by a reaction with excess HBF_4. The structure of the protonated **DpCy7** (**DpCy7**@H^+) was characterized by ^{1}H-NMR, ^{13}C-NMR and ESI-MS. The spectra are shown in Fig. S10–S13 (ESI†).

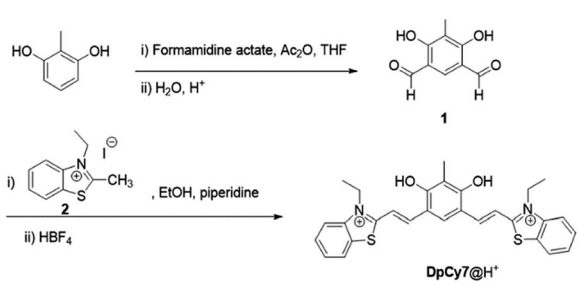

Scheme 1 The synthesis route of the protonated **DpCy7**.

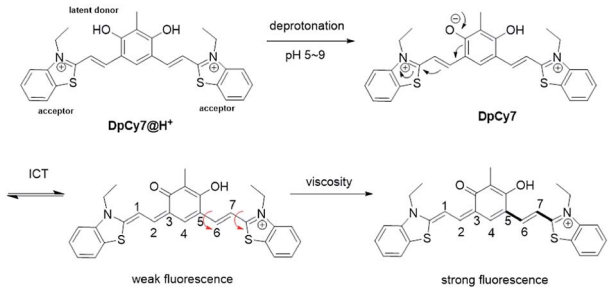

Scheme 2 Proposed structure conversions of **DpCy7** under different pH conditions (red arrow is the rotatory unit).

Photophysical properties of DpCy7

The dye **DpCy7** was designed so that a deep-red fluorescence was obtained upon removal of a proton in viscous medium, and so the spectroscopic properties of **DpCy7** were firstly studied in deionized water with and without 50% glycerol under different pH conditions. As shown in Fig. 1 and S1 (ESI†), the UV-vis and the fluorescence spectra of **DpCy7** in deionized water showed two main absorption maxima (*ca.* 450 nm and *ca.* 577 nm) and a weak emission peak (*ca.* 670 nm) upon excitation at 570 nm. When the value of the pH was controlled in the range of pH 1.0–4.0, the dominant absorption band was at about 450 nm, indicating that **DpCy7** remained in a protonated dicationic diphenol form **DpCy7**@H^+ (Scheme 2). With the increase of pH value up to the range of 5.0–9.0, enhancement of the absorbance at 577 nm was observed (Fig. S2, ESI†), which implied that it remained in a monocationic Cy7-like keto form in the weak acid and neutral environment. Moreover, the fluorescence behaviors of **DpCy7** in response to viscosity supported our prediction. As shown in Fig. S1c (ESI†), compared with the weak emission in water, a strong fluorescence emission in the deep-red region at

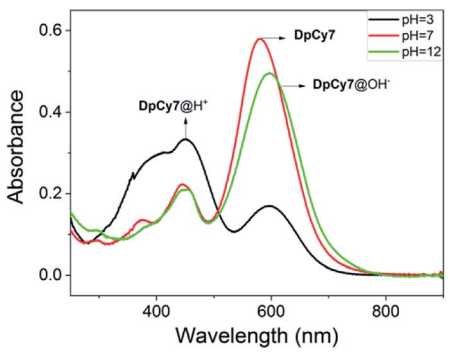

Fig. 1 UV absorption spectra of the dye **DpCy7** (10 μM) in aqueous solution with different pHs.

675 nm appeared in a 50% glycerol aqueous solution and the intensity of emission was almost steady in the pH range of 5.0–9.0. Simultaneously, a pink fluorescence was observed from corresponding viscous solutions in a 1 cm quartz cell under UV irradiation (inset of Fig. S1c, ESI†). The viscosity sensing property of **DpCy7** demonstrated that the phenolate form of **DpCy7** underwent an ICT process and emitted a deep-red fluorescence when free rotation between cationic benzothiazene and the styryl unit was restricted by the viscous environment. Next, when the solution medium was modulated to pH > 10.0, it was found that the maximum absorption band of **DpCy7**@OH^- appeared with *ca.* 20 nm bathochromic-shift (597 nm, pH = 11.0–12.0). But the intensity of the emission band obviously diminished both in absolute water and in 50% glycerol aqueous solution. This change may be due to the fact that the secondary deprotonation of **DpCy7** had occurred, which resulted in the formation of two donor moieties instead of the donor–acceptor pair fluorochrome supposed in **DpCy7** (Fig. S2a, ESI†). These pH-dependent structure transformations were supported by the results of ^{1}H-NMR controlled titrations of **DpCy7**@H^+ with NaOH in DMSO-d_6. As shown in Fig. S2b (ESI†), it was noted that the 'a' protons on the $-CH_2-$ group with the nitrogen atoms of indole salts as neighbors were obviously upfield shifted from 4.81 ppm to 4.64 ppm with the increase of pH value. Compared with an absorption peak that appeared in the region of 4.5–5.0 δ in **DpCy7**@H^+ (at 4.81 ppm) or in **DpCy7**@OH^- (at 4.64 ppm), the spectrum of **DpCy7** showed two peaks at 4.81 and 4.64 ppm, indicating that two nitrogen atoms adjacent to the 'a' protons in **DpCy7** were in different electronic environments. These results provided the evidence that **DpCy7** had formed a donor–acceptor pair fluorochrome, whereas **DpCy7**@H^+ and **DpCy7**@OH^- were transformed into less fluorescent structures with two acceptor moieties or two donor moieties in more acidic or basic conditions.

Considering the pH related properties of **DpCy7**, the absorbance changes in aqueous solution were analyzed according to eqn (1).[17] The dye **DpCy7** had pK_{a_1} of 4.1 corresponding to the conversion between **DpCy7**@H^+ and **DpCy7**, and a pK_{a_2} of 11.0 corresponding to the conversion between **DpCy7** and the deprotonation of **DpCy7** (Fig. S3, ESI†). Therefore, the dye **DpCy7** remained in a stable keto form in the physiological pH range (5.0–9.0), implying that **DpCy7** could be used for viscosity determination under physiological conditions.

$$\log[(A_{max} - A)/(A - A_{min})] = pH - pK_a \quad (1)$$

To further characterize the spectroscopic properties of **DpCy7**, different solvents including DMSO, tetrahydrofuran (THF), dichloromethane, methanol, water (H_2O), Ac_2O and glycerol were used to evaluate the solvent dependency of absorption and emission [Fig. S4 (ESI†) and 2]. It was found that the intermolecular hydrogen bonding affected the spectra of **DpCy7** to some extent. Most notably, the absorption maxima of **DpCy7** underwent hypochromic shifting from 667 nm in DMSO to 577 nm in water and the Stokes shift increased from 33 nm in DMSO to 93 nm in water (Table S1, ESI†). This observation may be explained by the fact that non-viscous protic solvents could

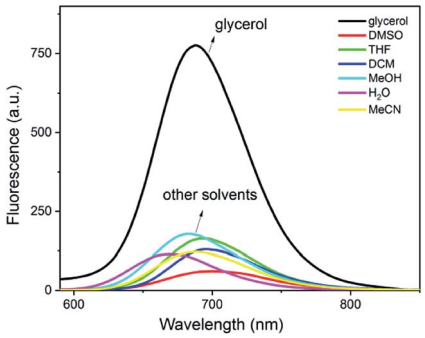

Fig. 2 Fluorescence spectra of **DpCy7** (5 μM) in various freshly prepared solvents. The solvents included: DMSO, tetrahydrofuran, dichloromethane, methanol, H_2O, acetonitrile and glycerol.

stabilize the phenoxide ion of **DpCy7**, thereby increasing the energy difference between the excited and ground states of **DpCy7**.[18] For the emission spectra, the quantum yield was not only influenced by polarity and H-bonding, but it was also sensitive to solution viscosity. The dye exhibited the highest quantum yield in a high viscous glycerol solution (Φ = 0.39 in glycerol, Φ = 0.13 in methanol, Φ = 0.05 in H_2O, Φ = 0.08 in DMSO) (Table S1, ESI†). These results indicated that the polarity and H-bonding of the solvents had a very weak effect on the fluorescence emission. Thus it was confirmed that the dye **DpCy7** could be used for monitoring the fluorescence changes of the viscosity.

Computational study

To better understand the photochemical properties of **DpCy7** under different pH conditions, density functional theory (DFT) calculations were carried out using a suite of Gaussian 09 programs (B3LYP/6-31G (d) basis sets).[11a] As shown in Fig. 3, the optimized structures in the ground states of **DpCy7**@H^+ and **DpCy7** illustrated that the monocationic keto form, **DpCy7** had a larger conjugated backbone between the two acceptor units than the protonated dicationic form, **DpCy7**@H^+. The HOMO distributions in **DpCy7** were delocalized over an aromatic ring, forming the larger π-extended conjugation. But the conjugated backbone in **DpCy7**@H^+ was partially interrupted by an aromatic ring, which was also evident by its weak fluorescence.

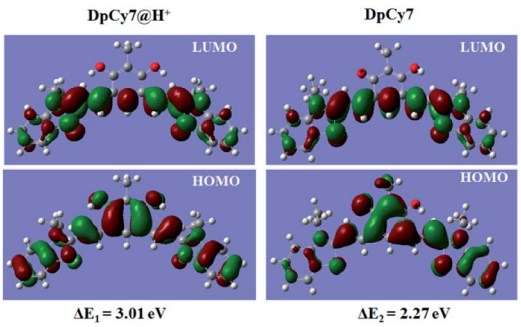

Fig. 3 The DFT optimised frontier orbital pictures of **DpCy7**@H^+ and **DpCy7**.

With increasing pH value, the HOMO and LUMO energies were both increased. Furthermore, the calculated transition energy ΔE of **DpCy7**@H^+ and **DpCy7** were 3.01 eV and 2.27 eV (Table S2, ESI†), respectively. This leads to the bathochromic-shift of the maximum absorption wavelength from 450 nm (**DpCy7**@H^+) to 577 nm (**DpCy7**) and fluorescence enhancement. The calculations were consistent with the experimental results.

Response of the fluorescence spectra of DpCy7 to viscosity

To further investigate its use as a molecular rotor for viscosity, the fluorescence changes of **DpCy7** as a function of the solvent viscosity were studied in water–glycerol mixture solutions of different proportions. In Fig. 4, **DpCy7** exhibited strong fluorescence in glycerol at 688 nm. With an increase of the ratio of glycerol to water from 1.0 cP (water) to *ca.* 1412 cP[19] (100% glycerol), the fluorescence of **DpCy7** exhibited an 8.5-fold enhancement with a large Stokes shift (from 93 nm to 73 nm). In addition, a good linear relationship was obtained between the logarithm of the fluorescence intensity ($\log I$) and the logarithm of the viscosity ($\log \eta$) ($R^2 = 0.992$, $b = 0.57$, $c = 1.79$) within the range of concentration from 1.0 cP to 60.1 cP (0–80% glycerol), which was consistent with the Förster–Hoffmann equation[20] (eqn (2); inset of Fig. 4). For practical applications, **DpCy7** was used to predict the viscosity of ethylene glycol. The fluorescence spectrum of **DpCy7** (5 μm) was then measured in absolute ethylene glycol (Fig. S5, ESI†). According to the linear relationship between $\log I_{688}$ and $\log \eta$ shown in the inset of Fig. 4, the logarithm of experimental viscosity ($\log \eta$) of ethylene glycol was calculated to be 1.169. Compared to the calculated $\log \eta$ (1.244) of ethylene glycol,[20] the error of the viscosity was about 6% (Table S3, ESI†). Thus the **DpCy7** rotor can function as a practical fluorescent probe to detect of the viscosity of viscous solutions.

$$\log I_{em} = c + b \log \eta \quad (2)$$

The photostability of **DpCy7** (5 μM) in the absence and presence of 50% glycerol was also evaluated. The **DpCy7** exhibited a relatively stable fluorescence output under a continuous wavelength of 570 nm laser excitation for 30 min (Fig. S6, ESI†). These results suggested that **DpCy7** had good photostability, and could be used as a fluorescent probe for quantitative detection of environmental viscosity.

Fluorescence lifetime measurement

As the fluorescence lifetime is an important response signal to the viscosity of the solvents, with no interference from fluorescence intensity and fluorophore concentration,[14b] it was more convenient to measure the fluorescence lifetime instead of the fluorescence intensity. Subsequently, the fluorescence lifetime of **DpCy7** in media of different viscosities were explored. As shown in Fig. 5, the lifetime was prolonged from 1.0712 ns to 1.8970 ns when the ratio of glycerol increased from 10% to 100%. A linear relationship was also obtained between the logarithm region of the fluorescence lifetime ($\log \tau$) and viscosity ($\log \eta$) ($R^2 = 0.996$) in the range of 10–60% glycerol (inset of Fig. 5). As a result, **DpCy7** could be used as a versatile deep-red fluorescence platform for sensing viscosity within wide viscous ranges *via* both turn-on and fluorescence lifetime modes.

The selectivity of DpCy7

In order to utilize the **DpCy7** rotor as a mitochondrial viscosity sensor, some reactive oxygen species and biological relevant species were chosen as mitochondrial interfering substances to carry out a controlled trial. Unlike the significant response to viscous media, **DpCy7** gave little response to the analytical species, especially anions (Fig. S7, ESI†). In the presence of interfering species, such as Cl^-, ClO^-, Cys, GSH, H_2O_2, Hcy, HSO_3^-, HSO_4^-, SO_3^{2-}, and SO_4^{2-}, there were no obvious influences on the fluorescence intensity at 688 nm. This provided evidence that in a complex biological system the **DpCy7** probe could potentially be used to detect viscosity variation as a molecular rotor.

Fluorescence imaging of the DpCy7 probe in living cells

To further investigate the application of the probe in biological systems, the MTT experiment was carried out to assess the cytotoxicity of **DpCy7**. After HeLa cells were incubated with various concentrations of **DpCy7** for 24 h, the high cell viability

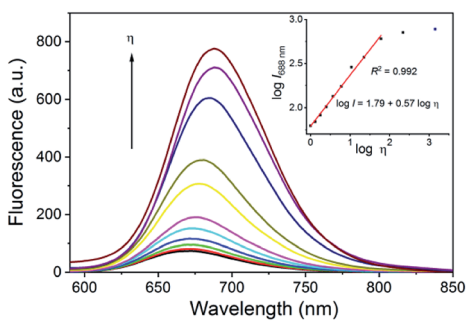

Fig. 4 Fluorescence spectra of **DpCy7** (5 μM) in different ratios of glycerol–water solutions. Inset: the linear relationship between log (I_{688}) and log (viscosity) in the glycerol–water solutions.

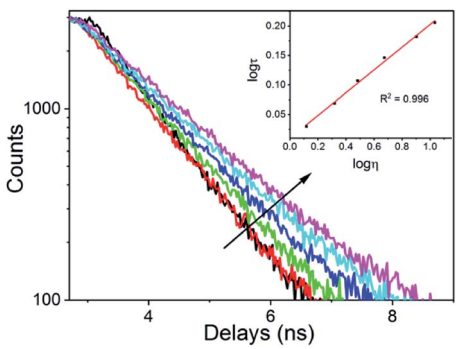

Fig. 5 Fluorescence lifetime of the **DpCy7** (5 μM) probe with changes of viscosity of the solution (10–60% glycerol) at 670 nm.

percentages (≧80%) were observed (Fig. S8, ESI†), illustrating that **DpCy7** was less cytotoxic. Subsequently, an attempt was made to monitor the viscosity changes of mitochondria stimulated by well-known ionophores, *e.g.*, monensin and nystatin,[13b] by **DpCy7**. As shown in Fig. 6, when the HeLa cells were treated with the **DpCy7** probe, there was a very weak red fluorescence. In comparison, the HeLa cells exhibited a strong red fluorescence in the **DpCy7** channel upon treatment with monensin or nystatin. It is known that the ion pores can cause the disruption of mitochondrial structure or the swelling of mitochondria by perturbation of the ionic balance, resulting in cell viscosity variation.[21,22] So it was reasonable to expect that the turn-on fluorescence imaging behaviors of the probe were not only sensitive to cell viscosity variation but also able to target mitochondrial locations. To confirm this hypothesis, the **DpCy7** probe was incubated with monensin together with addition of various co-localization agents, such as the mitochondrial kit Mito-TG, lysosome kit Lyso-TG and endoplasmic reticulum kit ER-TG, in HeLa cells for co-localization experiments. As shown in Fig. 7, the merged image reveals that the fluorescence of the cells stained by **DpCy7** overlapped very well with those stained with MitoTracker Green. The Pearson's co-localization coefficient (0.91) between **DpCy7** and Mito-TG was larger than the coefficients for Lyso-TG (0.47) and ER-TG (0.66) (Fig. S9, ESI†). The high correlation relationship illustrated that the probe **DpCy7** was mainly localized in the mitochondria rather than the lysosome or endoplasmic reticulum. All the previous results indicated that **DpCy7** was similar to traditional cyanine dyes with a positive charge and it could easily enter the negatively charged mitochondrial membrane on the surface of the membrane and turn-on fluorescence response to viscosity variation in the presence of stimuli agents. Therefore, the **DpCy7** probe should be suitable for applications to verify the change of mitochondrial viscosity in living cells.

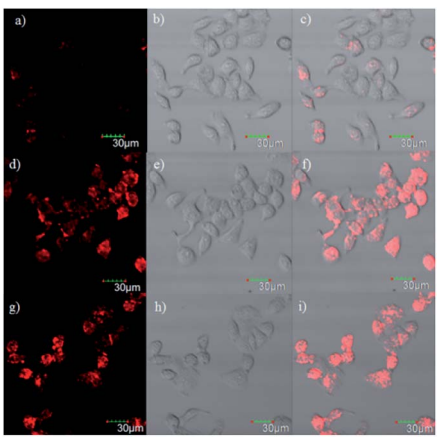

Fig. 6 Confocal microscopy images of HeLa cells. (a) Incubation with 1 μM **DpCy7** for 30 min; (b) bright field microscopy; (c) overlay of (a) and (b); (d) incubation with 1 μM **DpCy7** and 10 μM monensin for 30 min. (e) Bright field microscopy; (f) overlay of (d) and (e); (g) incubation with 1 μM **DpCy7** and 10 μM nystatin for 30 min; (h) bright field microscopy; (i) overlay of (g) and (h); λ_{ex} = 559 nm, λ_{em} = 600–700 nm; scale bar = 30 μm.

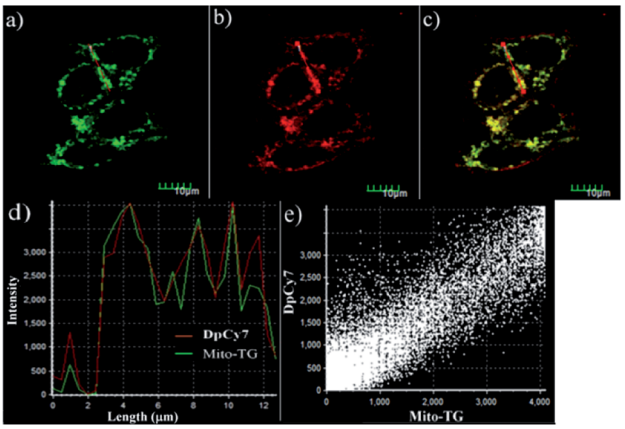

Fig. 7 Co-localization experiments involving the **DpCy7** probe (0.1 μM) and MitoTracker Green in HeLa cells incubated with 1 μM monensin at 37 °C for 30 min. (a) Confocal image from MitoTracker Green (200 nM) on green channel; (b) confocal image from 0.1 μM probe **DpCy7** on red channel; (c) merged image of (a) and (b); (d) the intensity profile of ROI lines; (e) fluorescence intensity dot plot of MitoTracker Green channel and **DpCy7** channel. Scale bar = 10 μm.

Conclusions

In conclusion, a novel deep-red fluorescence dye **DpCy7** with a molecular rotor structure has been designed and prepared by the condensation of diphenol-dialdehyde **1** with benzothiazole derivatives. The **DpCy7** possessed a donor-two-acceptor (D2A) π electron system, and can undergo an ICT process to form a new donor–acceptor system with a longer conjugated system. Because of the free rotation of a single bond between the cationic benzothiazole moiety and styryl unit, deep-red emission of **DpCy7** was observed in viscous medium. In the viscous medium, the fluorescence intensity of **DpCy7** was enhanced with the increase of the glycerol ratio, which was fitted with the Förster–Hoffmann equation with a large Stokes shift. Furthermore, confocal images of HeLa cells indicated that the **DpCy7** can enter cells and cause a light-up fluorescence response to the mitochondrial viscosity changes caused by various stimuli. Therefore, the molecular rotor **DpCy7** can be used as a potential probe for monitoring the changes of mitochondrial viscosity in live cells.

Experimental

Synthetic procedures

Synthesis of 2,4-dihydroxy-3-methylisophthalaldehyde (1). 2,4-Dihydroxy-3-methylisophthalaldehyde **1** was synthesized according to a previous method reported in the literature.[16] ^{1}H-NMR (DMSO-d_6, 400 MHz), δ (ppm): 11.93 (s, 2H), 9.94 (s, 2H), 8.20 (s, 1H), 2.05 (s, 3H).

Synthesis of the protonated DpCy7. A mixture of commercially available 3-ethyl-2-methylbenzothiazolium iodide (**2**, 610 mg, 2 mmol, 2 equiv.) and isophthalaldehyde **1** (179 mg, 1 mmol, 1 equiv.) was dissolved in EtOH (10 mL). Two drops (about 40 μL) of piperidine were added. The reaction mixture

was stirred at 95 °C under an argon atmosphere for 24 h. After completion of the reaction, the mixture was cooled to room temperature, 100 μL of HBF_4 was added, and the reaction was stirred at room temperature for 6 h. The reaction mixture was concentrated by evaporation under reduced pressure. The crude product was recrystallized from dichloromethane/diethyl ether to afford the desired protonated **DpCy7** as a dark blue solid (483 mg, 71.2% yield). HRMS: m/z $[M–2BF_4^-]^{2+}$ = 250.0822; calc'd for $[M–2BF_4^-]^{2+}$: 250.0791; ^{1}H-NMR (DMSO-d_6, 400 MHz), δ (ppm): 8.41 (s, 1H), 8.29 (d, J = 8.0 Hz, 2H), 8.22 (d, J = 15.6 Hz, 2H), 8.17 (d, J = 8.4 Hz, 2H), 7.95 (d, J = 15.2 Hz, 2H), 7.81 (t, J = 7.8 Hz, 2H), 7.71 (t, J = 7.6 Hz, 2H), 4.82–4.79 (m, 4H), 2.10 (s, 3H), 1.50 (t, J = 7.0 Hz, 6H); ^{13}C-NMR (DMSO-d_6, 100 MHz), δ (ppm): 171.8, 145.4, 141.4, 129.8, 128.4, 128.1, 124.7, 116.8, 116.6, 113.6, 110.0, 44.6, 14.4, 10.1.

Fluorescence lifetime measurement

The test solution was prepared by mixing deionized water–glycerol in different ratios. The fluorescence decay from the solution samples was measured with an Edinburgh Instruments FLS1000 steady state transient fluorescence spectrometer with excitation at 460 nm and emission at 670 nm.

Cytotoxicity assay

To assess the toxicity of **DpCy7** in living cells, HeLa cells were treated with different concentrations of the probe in DMEM medium supplemented with 10% fetal bovine serum (FBS) and allowed to grow for 24 h at 37 °C with 5% CO_2. After removal of the medium, cells in each well were treated with 10 μL MTT solution (5 mg mL^{-1}), and incubated for 4 h. Before taking the measurements, cells were treated with 100 μL DMSO at 37 °C for 1 h, and then the OD490 data for each well were recorded on a PL-9602 microplate reader immunoassay analyzer. The cell viability was calculated by using the formula: (experiment group − background)/(blank group − background) × 100%, and the survival rate of the cells can be calculated and the toxicity of the probe can be determined.

Imaging of viscosity in HeLa cells

The HeLa cells were cultured with a mixed solution of DMEM medium containing 10% FBS. The experimental environmental conditions were kept at 37 °C in a 5% CO_2. Before imaging, some of the adherent cells were incubated with 1 μM monensin or nystatin for 30 min, then washed three times with PBS (10 mM, pH = 7.4) before incubating with **DpCy7** for another 30 min, then the cells were again washed three times with PBS, and then images were taken with a confocal fluorescence microscope.

Conflicts of interest

There are no conflicts to declare.

Acknowledgements

We gratefully acknowledge the National Natural Science Foundation of China (NSFC 21907075, 21272172), and the Natural Science Foundation of Tianjin City (19JCZDJC32400, 18JCQNJC75900).

Notes and references

1 (*a*) Z. Yang, J. Cao, Y. Yang, T. Kim, X. Peng and J. S. Kim, *Chem. Soc. Rev.*, 2014, **43**, 4563; (*b*) T. D. Ashton, K. A. Jolliffe and F. M. Pfeffer, *Chem. Soc. Rev.*, 2015, **44**, 4547.
2 (*a*) D. Su, C. L. Teoh, L. Wang, X. Liu and Y. T. Chang, *Chem. Soc. Rev.*, 2017, **46**, 4833; (*b*) X. Li, X. Gao, W. Shi and H. Ma, *Chem. Rev.*, 2014, **114**, 590; (*c*) H. Kim and B. Cho, *Chem. Rev.*, 2015, **115**, 5014.
3 (*a*) X. Peng, F. Song, E. Lu, Y. Wang, W. Zhou, J. Fan and Y. Gao, *J. Am. Chem. Soc.*, 2005, **127**, 4170; (*b*) J. L. Zhao, Y. Lv, H. J. Ren, W. Sun, Q. Liu, Y. L. Fu and L. Y. Wang, *Dyes Pigm.*, 2013, **96**, 180.
4 (*a*) S. Zhu, R. Tian, A. L. Antaris, X. Chen and H. Dai, *Adv. Mater.*, 2019, **31**, 1900321; (*b*) Z. Guo, S. Park, J. Yoon and I. Shin, *Chem. Soc. Rev.*, 2014, **43**, 16.
5 (*a*) J. Chen, W. Liu, B. Zhou, G. Niu, H. Zhang, J. Wu, Y. Wang, W. Ju and P. Wang, *J. Org. Chem.*, 2013, **78**, 6121; (*b*) Q. Li, W. M. Liu, J. Wu, B. Zhou, G. Niu, H. Zhang, J. Ge and P. Wang, *Spectrochim. Acta, Part A*, 2016, **164**, 8.
6 L. Yuan, W. Lin, K. Zheng and L. He, *Chem. Soc. Rev.*, 2013, **42**, 622.
7 S. Kamino, M. Murakami, M. Tanioka, Y. Shirasaki, K. Watanabe, J. Horigome, Y. Ooyama and S. Enomoto, *Org. Lett.*, 2014, **16**, 258.
8 (*a*) X. Wu, S. Chang, X. Sun, Z. Guo, Y. Li, J. Tang, Y. Shen, J. Shi, H. Tian and W. Zhu, *Chem. Sci.*, 2013, **4**, 1221; (*b*) M. Vendrell, A. Samanta, S. Yun and Y. Chang, *Org. Biomol. Chem.*, 2011, **9**, 4760; (*c*) P. Choi, K. Noguchi, M. Ishiyama, W. A. Denny and J. Jose, *Bioorg. Med. Chem. Lett.*, 2018, **28**, 2013; (*d*) R. Guo, J. Yin, Y. Ma, G. Li, Q. Wang and W. Lin, *Sens. Actuators, B*, 2018, **71**, 321.
9 (*a*) S. Zhu, R. Tian, A. L. Antaris, X. Chen and H. Dai, *Adv. Mater.*, 2019, **31**, 1900321; (*b*) X. Cao, J. Liu, P. Hong, G. Li and C. Hao, *J. Photochem. Photobiol., A*, 2017, **346**, 444.
10 W. Sun, S. Guo, C. Hu, J. Fan and X. Peng, *Chem. Rev.*, 2016, **116**, 7768.
11 (*a*) N. Karton-Lifshin, L. Albertazzi, M. Bendikov, P. S. Baran and D. Shabat, *J. Am. Chem. Soc.*, 2012, **134**, 20412; (*b*) E. Kisin-Finfer and D. Shabat, *Bioorg. Med. Chem.*, 2013, **21**, 3602; (*c*) Y. Yue, F. Huo, C. Yin, J. Chao and Y. Zhang, *Sens. Actuators, B*, 2015, **212**, 451; (*d*) N. Narayanaswamy, S. Das, P. K. Samanta, K. Banu, G. P. Sharma, N. Mondal, S. K. Dhar, S. K. Pati and T. Govindaraju, *Nucleic Acids Res.*, 2015, **43**, 8651.
12 (*a*) D. R. Green and J. C. Reed, *Science*, 1998, **281**, 1309; (*b*) H. Zhu, J. Fan, J. Du and X. Peng, *Acc. Chem. Res.*, 2016, **49**, 2115; (*c*) M. A. Haidekker and E. A. Theodorakis, *Org. Biomol. Chem.*, 2007, **5**, 1669.

13 (*a*) G. S. Zubenko, U. Kopp, T. Seto and L. L. Firestone, *Psychopharmacology*, 1999, **145**, 175; (*b*) Z. Yang, Y. He, J. H. Lee, N. Park, M. Suh, W. S. Chae, J. Cao, X. Peng, H. Jung and C. Kang, *J. Am. Chem. Soc.*, 2013, **135**, 9181.

14 (*a*) Y. Wu, W. Shu, C. Zeng, B. Guo, J. Shi, J. Jing and X. Zhang, *Dyes Pigm.*, 2019, **168**, 134; (*b*) X. Peng, Z. Yang, J. Wang, J. Fan, Y. He, F. Song, B. Wang, S. Sun, J. Qu and J. Qi, *J. Am. Chem. Soc.*, 2011, **133**, 6626; (*c*) S. M. Yarmoluk, V. B. Kovalska, S. S. Lukashov and Y. L. Slominskii, *Bioorg. Med. Chem. Lett*, 1999, **9**, 1677; (*d*) W. West, S. Pearce and F. Grum, *J. Phys. Chem.*, 1967, **71**, 1316.

15 (*a*) Z. Zou, Q. Yan, S. X. Ai, P. Qi, H. Yang, Y. F. Zhang, Z. H. Qing, L. H. Zhang, F. Feng and R. H. Yang, *Anal. Chem.*, 2019, **91**, 8574; (*b*) W. J. Zhang, R. T. K. Kwok, Y. L. Chen, S. J. Chen, E. G. C. Y. Y. Yu, J. M. Y. Lam, Q. C. Zheng and B. Z. Tang, *Chem. Commun.*, 2015, **51**, 9022.

16 S. H. M. Mehr, H. Depmeier, K. Fukuyama, M. Maghami and M. J. MacLachlan, *Org. Biomol. Chem.*, 2017, **15**, 581.

17 A. P. de Silva and T. E. Rice, *Chem. Commun.*, 1999, **2**, 163.

18 H. J. Chen, C. Y. Chew, E. H. Chang, Y. W. Tu, L. Y. Wei, B. H. Wu, C. H. Chen, Y. T. Yang, S. C. Huang and J. K. Chen, *J. Am. Chem. Soc.*, 2018, **140**, 5224.

19 Y. L. Wu, W. Shu, C. Y. Zeng, B. P. Guo, J. W. Shi, J. Jing and X. L. Zhang, *Dyes Pigm.*, 2019, **168**, 134.

20 A. R. Katritzky, K. Chen, Y. Wang, M. Karelson, B. Lucic, N. Trinajstic, T. Suzuki and G. Schüürmann, *J. Phys. Org. Chem.*, 2000, **13**, 80.

21 I. Lopez-Duarte, T. T. Vu, M. A. Izquierdo, J. A. Bull and M. K. Kuimova, *Chem. Commun.*, 2014, **50**, 5282.

22 W. Sun, Y. D. Shi, A. X. Ding, Z. L. Tan, H. Chen, R. Liu, R. Wang and Z. L. Lu, *Sens. Actuators, B*, 2018, **276**, 238.